CHINESE JOURNAL OF GEOCHEMISTRY Vol. 26 No. 4 2007

DOI: 10.1007/s11631-007-0356-4

Geochemistry of lamprophyres associated with uranium mineralization, Southeastern Desert, Egypt

Mohamed E. Ibrahim[1], Mohamed M. El-Tokhi[2*], Gehad M. Saleh[1], Mamdouh A. Hassan[1], and Mohamed A. Rashed[1]

[1] *Nuclear Materials Authority, P. O. Box 530 El Maadi, Cairo, Egypt*

[2] *Geology Deprtment, Faculty of Science, United Arab Emirates University, United Arab Emirates*

** Corresponding author, E-mail: meltokhi@mans.edu.eg*

Received August 14, 2006; accepted September 10, 2006

Abstract Two brecciated shear zones (NNW-SSE) are found crosscutting cataclastic rocks. The cataclastic rocks (3.0 km^2) occupy the core of the granitic pluton and enclose a roof pendant of mafic-ultramafic rocks. The NNW-SSE-extending lamprophyre dykes vary in thickness from 0.5 m to 1 m and up to 800 m long, cutting the cataclastic rocks and are composed mainly of plagioclases, amphiboles, relics of pyroxenes and K-feldspar phenocrysts embedded in fine-grained groundmass. They are characterized as being peraluminous, calc-alkaline in composition (chemical trap) and enriched in calcite, sulfide and P_2O_5.

The lamprophyres were affected by hydrothermal alteration (chlorite-carbonate alteration) while the cataclastic rocks were affected by diagenetic alteration (K-feldspar-albite alteration).

Uranium mineralization is the product of hydrothermal events and has been investigated by X-ray diffraction (XRD) and environmental scanning electron microscopy (ESEM), involving primary uranium minerals (U_3O_8) and secondary uranium minerals (uranophane and beta-uranophane, kasolite, torbernite, autonite and meta-autonite) in addition to U-bearing minerals (astrocyanite, betafite and fergusonite).

The presence of different mineral parageneses associated with clay minerals indicates that the lamprophyres were subjected to acidic and alkaline mineralizing solutions. Moreover, the U-Zr/U, U-Ce/U values show negative correlations, confirming U-enrichment in both cataclastic rocks and shear zones while the Th-eU/eTh, Th-Zr/Th and Th-Ce/Th values show negative correlations, indicating that the U-bearing solutions are rich in Th in the cataclastic rocks only.

Key words cataclastic rock; shear zone; lamprophyre; hydrothermal alteration; Southeastern Desert; Egypt

1 Introduction

The Abu Rusheid area is one of the most important areas in the Southeastern Desert with respect to its uranium mineralization. Hassan (1964 and 1973), Sabet et al. (1976), El-Gemmizi (1984), Eid (1986), Saleh (1997) and Ibrahim et al. (2000) carried out investigations in this area and revealed some mineralization [e.g. tantalum-niobium, zircon, thorite and secondary uranium minerals (uranophane and beta-uranophane)]. In this paper, we give some light on the U-mineralization and geochemistry of lamprophyres in the Abu Rusheid area.

2 Geological setting and petrography

The Abu Rusheid area is located about 45 km southwest of Marsa Alam Town, Southeastern Desert. Detailed geologic survey of the Abu Rusheid area (3.0 km^2) was conducted on a 20×20 m grid. The tectonostratigraphic sequence of the Precambrian rocks in the Abu Rusheid area (Fig. 1) is presented as follows: (1) Ophiolitic mélange, consisting of ultramafic rocks and layered metagabbros in metasedimentary matrix; (2) cataclastic group, consisting of protomylonites, mylonites, ultramylonites and silicified ultramylonites; (3) mylonitic granites; and (4) post-granite dykes and veins (Ibrahim et al., 2004).

The protomylonites are coarse- to very coarse-grained (>50 in vol.% porphyroclasts), green to dark greenish-grey in color. They outcrop on the eastward flank of West Abu Rusheid around Khour Abalea as elongated scattered bodies, accounting for about 12.0 in vol.% of the cataclastics. Mylonites cover a large area, amounting to 65.0 in vol.% of the cataclastic rocks with low to medium relief. Feldspathic arenites outcrop as small bands in alternation with mylonite

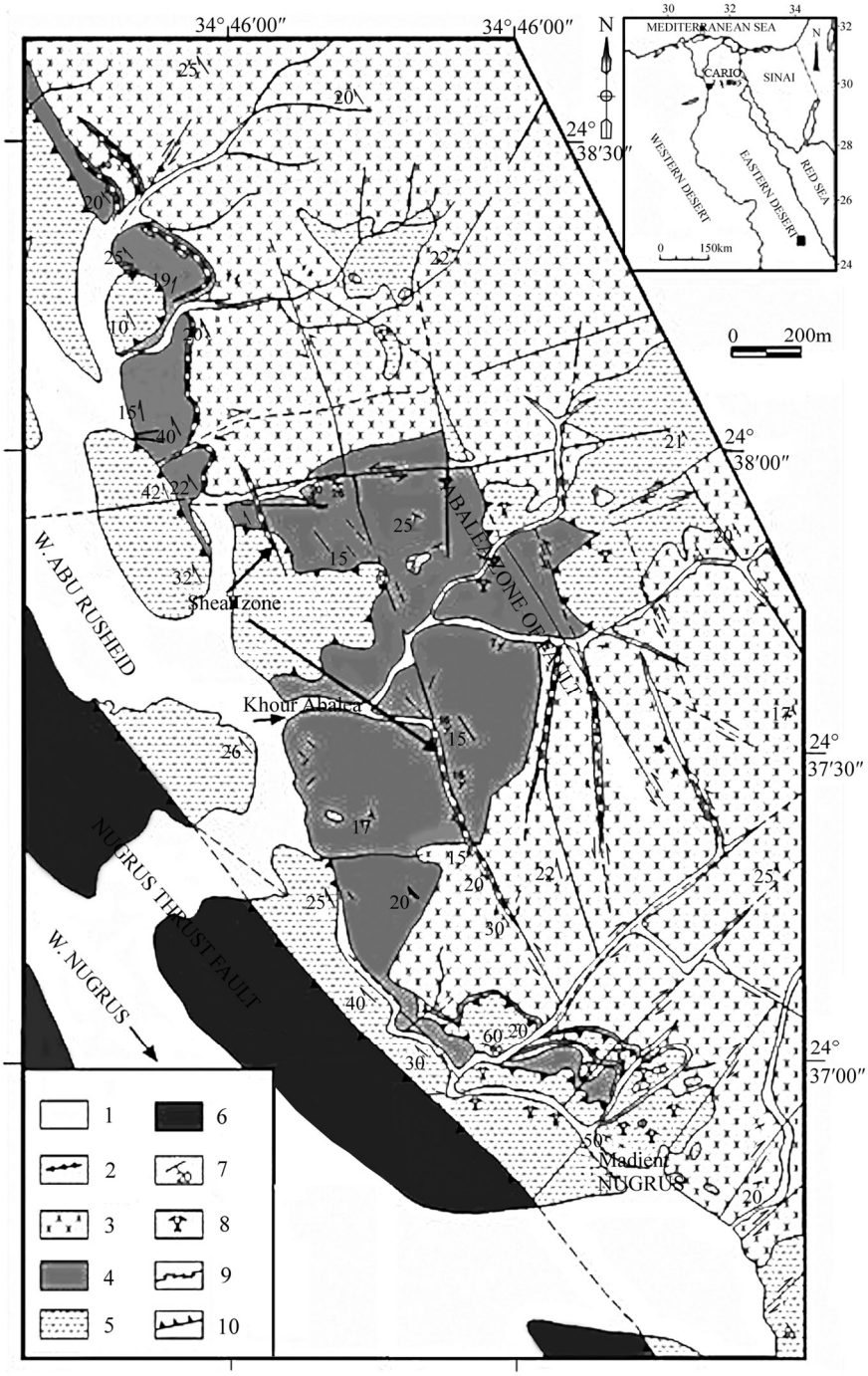

Fig. 1. Detailed geological map of the Abu Rusheid area, Southeastern Desert, Egypt (after Ibrahim et al., 2004). 1. Wadi deposit; 2. quartz vein; 3. granitic rock; 4. cataclastic rock; 5. ophiolitic melange; 6. metagabbro; 7. strike and dip of foliation; 8. ancient emerald mine; 9. fault; 10. thrust fault.

bands at the high relief of the third shear zone. They are medium-grained, well banded, and intercalated with protomylonite. Ultramylonites account for about 17.0 in vol.% of the cataclastic rocks. They are light grey to grey in color, fine- to medium-grained in size and exhibit both foliated and lineated gneissosity. Silicified ultramylonites account for about 6.0 in vol.% of the cataclastics with variable sizes (5–20 m) and shapes (irregular and oval), capping all the older rocks in the mapped area.

The cataclastic rocks of the Abu Rusheid area are cross-cut by two shear zones parallel to each other (NNW-SSE) and dissected by strike-slip faults with a minor displacement. Uranium mine-rals, iron oxides, zinc, clay minerals, fluorite and manga- nese oxides are present as thin films along fracture planes in the lamprophyres. The first shear zone resembles a V-shaped longitudinal trench, about 400 m far away from West Abu Rusheid, and extends about 800 m in length and approximately 5–20 m in width (Fig. 2a) and is overlain by approximately 50-m-thick flat- lying protomylonite and ultramylonite, followed up- wards by silicified ultramy- lonite (quartz >90 in vol.%). Seven trenches have been excavated through the first shear zone beginning from the south (T1) to the north (T7). The field observation revealed decreases in U contents and increases in Al_2O_3 (33%) and total iron (34%), especially in the southern part of the shear zone, whereas in its northern part mineralization (U & Cu) tends to become more visible, accompanied by a decrease in relief from south to north. Many vugs were formed in the first shear zone (especially in the close contact of the lamprophyres) as a result of leaching processes, and were filled by calcite, secondary quartz and uranium minerals. The second shear zone runs through mylonites with a relatively low relief, about 200 m far away from West Abu Rusheid, and parallel to the first shear zone, 280 m long in the NNW-SSE direction and approximately 2–10 m in width (Fig. 2b). Four trenches have been excavated beginning from the south (T8) to the north (T11). This

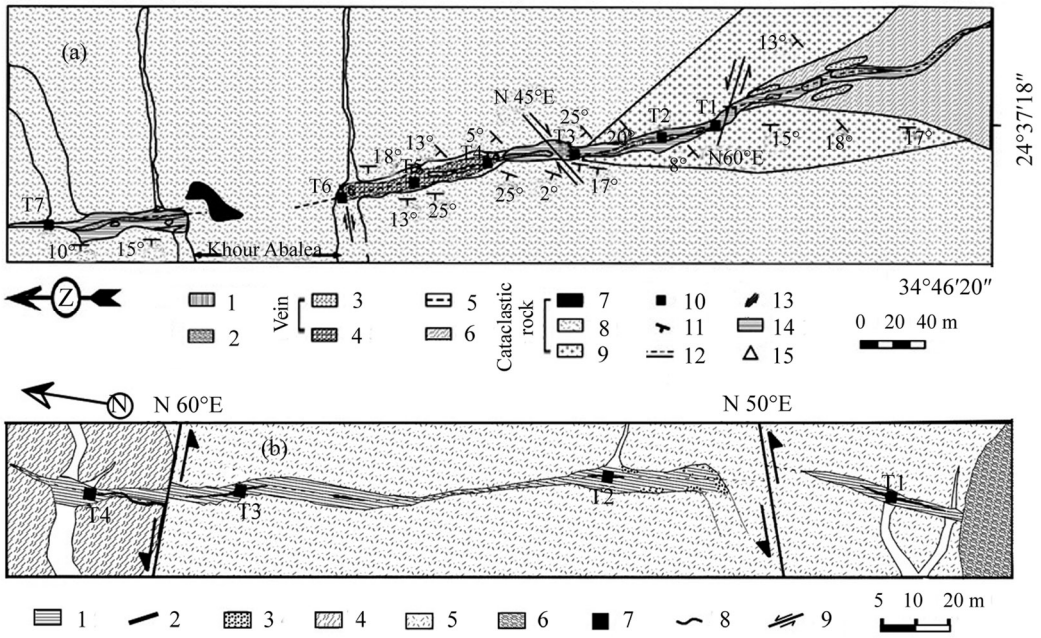

Fig. 2(a). Abu Rusheid shear zone No. I , Abu Rusheid area, SED, Egypt. 1. Alluvial sediment; 2. brecciated zone; 3. quartz-band; 4. pegmatite; 5. lamprophyre dyke; 6. biotite granite; 7. silicified ultramylonite; 8. ultramylonite; 9. protomylonite; 10. site of trench; 11. strike and dip foliation; 12. inferred, sharp contact; 13. strike-slip fault; 14. shear zone; 15. triangle point. 2(b). Abu Rusheid shear zone No.II, Abu Rusheid area, SED, Egypt. 1. Shear zone; 2. basic dyke; 3. pegmatite; 4. two mica granite; 5. mylonite; 6. ophiolitic melange; 7. trench site; 8. sharp contact; 9. strike-slip fault.

shear zone is characterized by the presence of pegmatite pockets which are dispersed along the southern part. The third shear zone (ENE-WSW) runs through mylonitic rocks at the contact with the two mica granites, perpendicular to the first two shear zones and West Abu Rusheid. It is 800 m long and 2–10 m wide. The mylonites are alternated with feldspathic arenite bands. The shear-zone rocks are fine- to medium-grained, highly brecciated, and characterized by different colors (black, whitish, pink and red), depending on the degree of metasomatic alteration such as kaolinization, silicification, flouritizaton, hematitization and greisenization. Greisenization is commonly seen in the first and third shear zones and represented by banded muscovite occurring at the contact between the cataclastic rocks and the lamprophyres.

3 Uranium mineralization

3.1 Primary uranium minerals

The primary uranium minerals are resultant from reduction reaction in the second shear zone and U_3O_8 was then formed, which was transported in solutions in the form of highly soluble uranyl ion (U^{6+}), and its precipitation occurred when the solutions found their way into a reducing environment, so the U_3O_8 has been formed by reduction of the earlier–formed uranyle phase (dehydrated schoepite, UO_3 0.8 H_2O). U_3O_8 is detected in the No. II shear zone of the Abu Rusheid area, as confirmed by XRD (Fig. 3a). U_3O_8 is easy to identify because it can be precipitated as yellow acicular aggregates of uranophane as a result of secondary alteration.

3.2 Secondary uranium minerals

In the Abu Rusheid area as well as in the oxidation zone, U^{4+} is oxidized to uranyl ion U^{6+} which is soluble and mobile in solutions and easy to combine with other cations such as Ca^{2+}, Cu^{2+} and Pb^{2+}, and anions such as those present in the form of sulphates and phosphates tend to form secondary uranium minerals such as uranophane, beta-uranophane, kasolite, torbernite, autunite and meta-autunite.

3.2.1 Uranophane and beta-uranophane ($CaO\ 2UO_3{\cdot}2SiO_2{\cdot}6H_2O$)

Uranophane occurs as hair-like, radiated, tuffed aggregates or crusts, or as coatings along fractures (Fig. 3b) which are also massive and usually dull, earthy to waxy dull in color. However, beta-uranophane is distinguished from uranophane by its yellowish-green color as observed under the reflected light microscope. It is waxy or greasy in luster and pale brown or brownish-yellow in streak. It also occurs as coatings along crevasses in igneous or

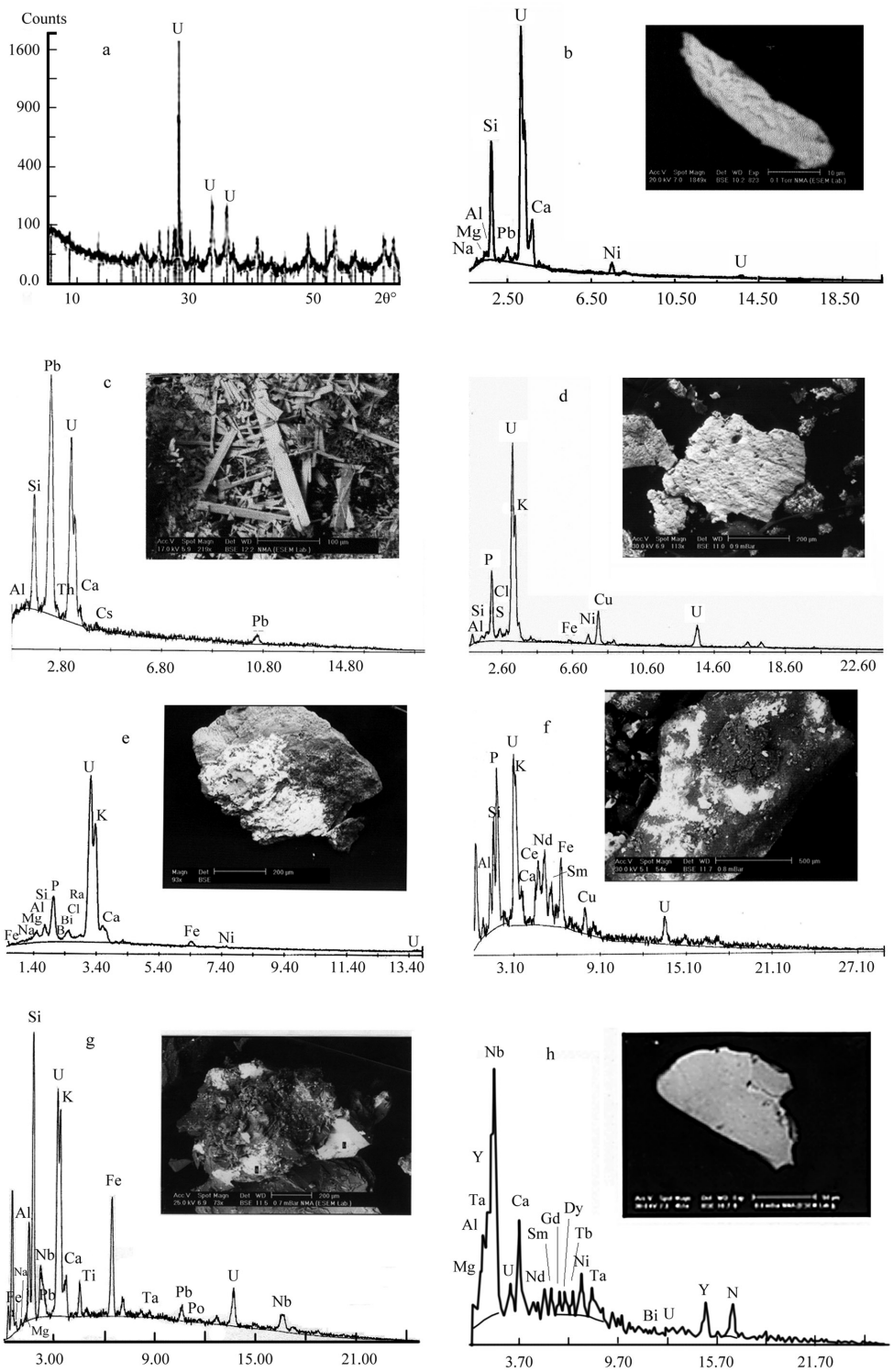

Fig. 3. XRD patterns of U_3O_8 from shear zone No.II, Abu Rusheid area (a); ESEM photomicrograph of uranophane (b); kasolite from shear zone No.II (c); ESEM photomicrograph of torgernite from shear zone Nos.I and II (d); autunite, from shear zone No.I (e); astrocyanite, from shear zone Nos.I and II (f); betafite, from shear zone Nos.I and II (g); and fergusonite, from shear zone Nos.I and II, Abu Rusheid area, SED, Egypt (h).

other rocks, without any close association with the primary uranium minerals. It seems to have been deposited from meteoric waters percolating through these fissures. Beta-uranophane is another secondary uranium mineral separated from the investigated rocks with the same mode of occurrence and association as its dimorph uranophane.

3.2.2 Kasolite [$Pb(UO_2)(SiO_3)(OH)_2$]

Kasolite was confirmed by ESEM (Fig. 3c) and XRD techniques and it contains 40% UO_2 and 53% PbO. This mineral generally occurs either as minute dispersions or micro-fracture infillings and coatings on surfaces of hematized joints. On the other hand, kasolite is distinguished by its yellowish-brown to reddish-orange colors.

3.2.3 Torbernite [$Cu(UO_2)_2(PO_4)_2 \cdot 8–12H_2O$]

Torbernite is common in shear zones I and II of the Abu Rusheid area and occurs as micaceous flakes of green color, as confirmed by ESEM (Fig. 3d). The mineral contains 74% UO_2, 11% CuO and minor amounts of Al_2O_3, Fe_2O_3, NiO_2 and P_2O_5.

3.2.4 Autunite & meta-autunite [$Ca(UO_2)_2(PO_4)_2 \cdot 8H_2O$] & [$Ca(UO_2)_2(PO_4)_2 \cdot 4–6\ H_2O$]

The autunite and meta-autunite have been detected in shear zone No. I of the Abu Rusheid area and occur as crusty aggregates of yellowish-green color. The minerals contain 23% P_2O_5, 25% UO_2 and the associated minerals contain 13% K_2O, 6.5% Bi_2O_3 and 5% CaO, as detected by ESEM (Fig. 3e).

3. 3 Uranium-bearing minerals

3.3.1 Astrocyanite (Ce) [$Cu_2(REE)_2(UO_2)(CO_3)_5(OH)_2 \cdot 1.5H_2O$]

The mineral occurs as grey bright flacks in shear zones I and II, adsorbed on clay minerals and composed mainly of UO_2=40%, CeO_3=14%, NdO_3=9.2%, Sm_2O_3=3.2% (∑REE=26.4%), P_2O_5=9.4%, and CuO=3.6%, as detected by ESEM (Fig. 3f).

3.3.2 Betafite [$(Ca,Na,U)_2\ (Nb,Ta)_2O_6 \cdot nH_2O$]

The mineral occurs as an alteration phase, brown to black in color, containing potential concentrations of high field strength elements (HFSE) such as Nb, Ta and Ti in addition to U. The chemical analysis data (UO_2=48%, Nb_2O_5=27%, CaO=1.1% and Ta=1.3%) were confirmed by SEM (Fig. 3g).

3.3.3 Fergusonite (Nb,Y,Ta,U, Al, Mg, REE)

Fergusonite is of tabular prismatic shape, as confirmed by ESEM (Fig. 3h).

4 Geochemistry

4.1 Analytical methods

Sixteen samples were analyzed on a Philips PW-2400 X-ray fluorescence spectrometer (XRF).The uncertainties of analyses are 1%–2% for the major elements and around 10% for the trace and REE elements. All chemical analyses were carried out in the Acme Analytical Laboratories LTD, Vancouver, Canada. The samples were crushed in a jaw crusher and powdered in an agate mill at the Egyptian Nuclear Materials Authority. The geochemistry data are presented in Tables 1 and 2).

Creasy (1959) classified the hydrothermally altered rocks as argillic facies (characterized by any member of the kaolinite group) and K-silicate facies (characterized by muscovite-biotite and K-feldspar). The argillic facies was further classified by Meyer and Hemley (1967) as advanced argillic (kaolinite and montmorillonite replacing plagioclases) and intermediate argillic (all the feldspars are converted to

Table 1. Representative major oxides (wt%) analyses of cataclaclastic and shear-zone rocks, Abu Rusheid area, Southeastern Desert, Egypt

Sample	Cataclastic rock										Shear zone						
	Protomylonite N=2	Mylonite N=3			Ultramylonite N=3			Silicified ultramylonite N=3			Lamprophyre N=5					Wall zone N= 2	
SiO_2	69.01 (69.90–68.12)	70.63	71.96	69.70	72.01	69.30	72.40	83.70	81.00	85.61	43.80	43.10	42.30	53.50	42.70	71.40	66.50
TiO_2	0.04 (0.06–0.02)	0.03	0.05	0.04	0.04	0.03	0.04	0.07	0.05	0.05	3.81	3.77	3.86	2.27	3.88	0.58	0.20
Al_2O_3	14.22 (14.3–14.13)	12.50	13.30	15.50	11.60	15.00	10.70	6.50	11.80	5.20	20.01	19.20	17.20	17.50	17.00	12.60	16.30
Fe_2O_3	3.0 (2.80–3.19)	2.40	1.60	2.00	1.99	2.00	3.19	3.99	1.60	3.19	16.80	17.60	20.00	11.98	20.00	3.99	4.00
MgO	0.07 (0.05–0.08)	0.10	0.01	0.01	0.02	0.01	0.02	0.02	0.01	0.02	0.02	0.01	0.01	0.06	0.02	0.06	0.05
MnO	0.83 (0.50–1.16)	1.00	1.20	0.25	1.12	0.50	2.00	0.80	0.50	0.40	1.50	0.50	1.00	1.50	0.50	0.80	0.22
CaO	1.17 (0.70–1.63)	0.80	0.50	1.05	1.20	0.50	0.56	0.60	0.70	1.12	0.70	1.40	1.40	2.10	2.10	1.12	1.40
Na_2O	5.45 (5.70–5.20)	6.00	6.10	5.90	5.23	4.80	5.13	1.00	1.40	0.54	0.50	0.47	0.50	0.47	0.50	2.77	4.50
K_2O	3.48 (3.01–3.95)	3.70	3.20	2.80	2.23	4.00	3.32	1.70	0.80	1.14	2.80	2.20	2.80	2.20	2.14	5.28	3.30
P_2O_5	1.4 (1.70–1.10)	1.70	1.23	1.60	3.03	2.20	2.20	1.18	1.60	0.38	1.90	2.30	1.90	0.25	2.10	0.06	1.70

Table 2. Trace element ($\times10^{-6}$) compositions of granite, drill core, cataclastic and shear-zone rocks, Abu Rusheid area, Southeastern Desert, Egypt

Trace element	Granite	Drill core	Cataclastic rock	Shear zone	
				Lamprophyre	Wall zone
	N=5	N=3	N=11	N=24	N=5
Ba	765 (210–1615)	293 (51–476)	60 (13–91)	204 (40–378)	130 (48–274)
Co	1.5 (0.7–2.3)	6.6 (3.5–16)	1.1 (1–19)	7 (1–37)	5.2 (1–11)
Cs	32.6 (0.2–6.8)	11.6 (6.5–19)	3.5 (2–7)	10 (1–50)	4.4 (1–8)
Ga	26.4 (21–32)	60 (36–72)	57 (13–69)	32 (15–59)	48 (34–59)
Hf	7.7 (1.1–12)	112 (13–263)	150 (10–240)	30 (6–184)	88 (9–163)
Nb	45 (9.6–79)	636 (73–1420)	739 (114–1174)	80 (55–140)	390 (82–774)
Rb	187 (27–312)	765 (263–1146)	682 (240–1274)	530 (154–927)	807 (550–1194)
Sn	23 (2–48)	539 (79–867)	220 (17–1083)	26 (20–82)	108 (63–280)
Sr	145 (62–288)	59 (13–93)	24 (4–58)	56 (10–89)	59 (25–80)
Ta	4 (1.5–8.2)	66 (7–164)	93 (12–150)	4 (3.3–6.2)	11 (5–18)
Th	9.8 (2.9–16.8)	123 (20–287)	133 (21–296)	40 (6–146)	160 (24–316)
U	4.8 (1.1–9)	43 (9–91)	53 (5–150)	440 (59–680)	139 (80–239)
W	17 (11–33)	54 (19–122)	16 (8–32)	146 (11–446)	60 (11–168)
Zr	246 (67.8–468)	1508 (371–2942)	2250 (80–3560)	678 (84–2470)	662 (291–2121)
Y	54 (14.2–84)	324 (116–718)	61 (8–162)	3770 (127–6139)	179 (28–354)

Note: N. Number of samples analyzed for trace elements ($\times10^{-6}$).

dickite and kaolinite) subtypes.

Meyer and Hemley (1967) classified the K-silicate facies as: (1) propylitic (containing epidote-chlorite alteration), (2) sericitic (containing plagioclases and K-feldspars, both of which were converted to sericite) and (3) potassic (characterized by the alteration of plagioclase into K-feldspar or mafic minerals into muscovite) subtypes.

Cataclastic and shear-zone samples are plotted on the AKF ternary diagram (Fig. 4) (after Meyer and

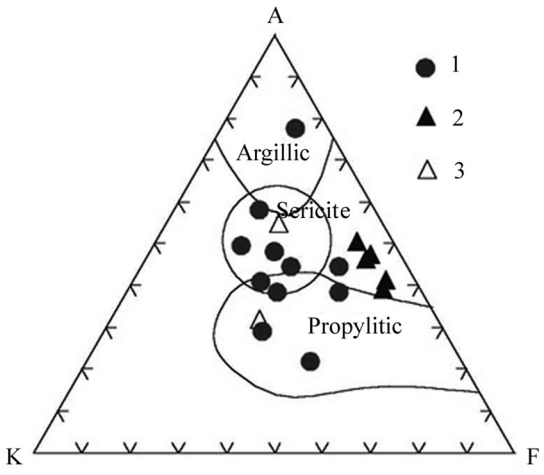

Fig. 4. AKF ternary diagram after Meyer and Hemley (1967). $A=Al_2O_3-(Na_2O+K_2O)$; $K=K_2O$; and $F=FeO+MnO+MgO$; Abu Rusheid area, SED, Egypt. 1. Cataclastic rock; 2. lamprophyre sample; 3. wall zone.

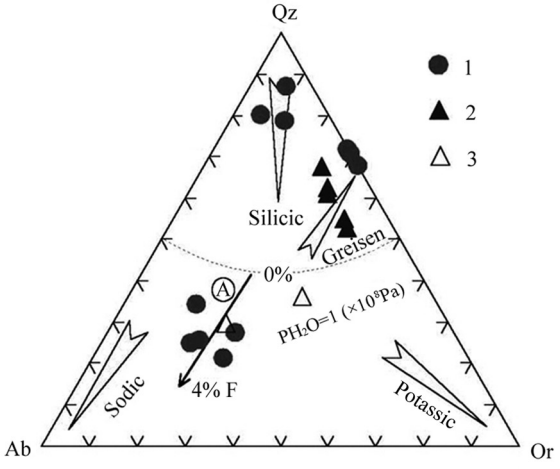

Fig. 5. Normative QZ-Ab-Qr ternary diagram of the Abu Rusheid area. The ternary minimum for 1kb H_2O pressure from Tuttle and Bowen (1958) and Manning (1981). Vector A shows the migration of ternary minima as F contents increase in the melt. The trends of granitic alteration types are from Stemprok (1979), Abu Rusheid area, SED, Egypt. 1. Cataclastic rock; 2. lamprophyre sample; 3. wall zone.

Hemley, 1967), where $A=Al_2O_3-(Na_2O+K_2O)$, $K=K_2O$ and $F=FeO+MnO+MgO$. It is shown that six of the cataclastic samples fall in sericite facies (due to sericitization processes) except three samples fall in the propylitic field and one sample falls in the argillic field. Whereas the shear-zone samples are close to the AF line, but beyond the fields of sericite and propylitic because of their high contents of Al_2O_3+FeO. Only one sample lies in the sericite field and the other one lies in the propylitic field.According to the normative Qz-Ab-Or compositions, the cataclastic samples could be classified as sodic, potassic, silicic and greisen types as shown in (Fig. 5) after Stemprok (1979). The cataclastic samples lie closely to the Ab and silicic trends whereas the shear zone samples lie in the greisen trend, while two cataclastic (wall-zone) samples lie below the granitic eutectic temperature.

The alteration is a graphical representation that uses two alteration indices: the Ishikawa alteration index (AI)=100 $(K_2O+MgO)/(K_2O+MgO+Na_2O+CaO)$ and the chlorite carbonate pyrite index (CCPI)=100 $(MgO+FeO)/(Mgo+FeO+Na_2O+K_2O$ (Large et al., 2001). The Ishikawa (AI) index was defined by Ishikawa et al. (1976) to quantify the intensity of sericite and chlorite alterations. The key reactions measured by the index involve the breakdown of sodic plagioclase and replacement by sericite and chlorite. Reactions that describe these alteration processes include:

$$3NaAlSi_3O_8+K^++2H^+ \text{ (Albite)} = KAl_3Si_3O_8(OH)_2+6SiO_2+3Na^+ \quad (1)$$

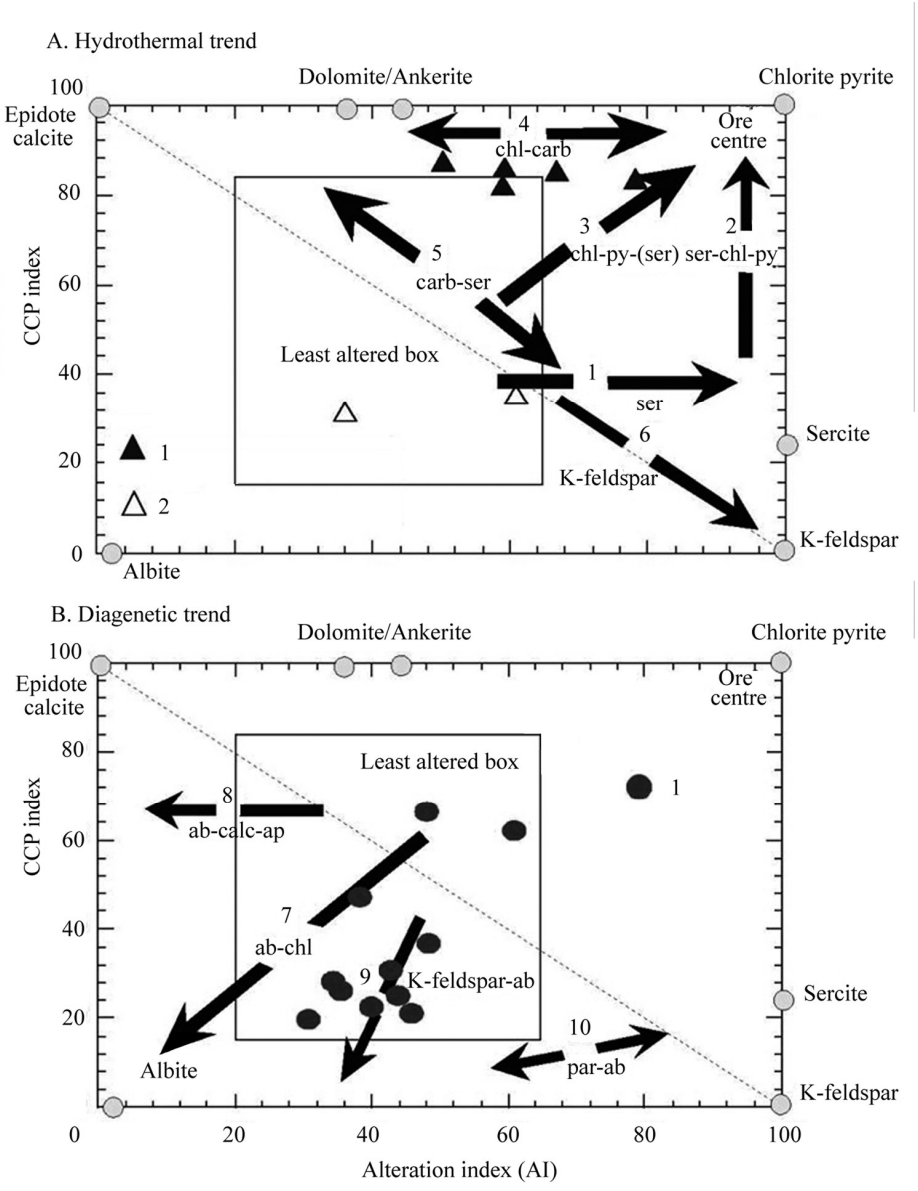

Fig. 6A and B. A hydrothermal and diagenetic alteration box plots (after Large et al., 2001). Trend No. 9 (after Gifkins and Allen, 2001), Aub Rusheid area, SED, Egypt. ▲ Lamprophyre sample; △ wall zone.

Sericite Quartz

$$2KAl_3Si_3O_{10}(OH)_2+3H_2SiO_4+9Fe^{2+}+6Mg^{2+}+18H_2O$$

Sericite

$$=3Mg_2Fe_3Al_2Si_3O_{10}(OH)_8+2K^++28H^+ \quad (2)$$

Chlorite

The first reaction is typical of sericite replacement of albite (Date et al., 1983 and Eastoe et al., 1987). The second reaction is so important that it is closely related to massive sulfide mineralization where chlorite-rich assemblages become dominant over sericite-rich assemblages (Lentz, 1999). Reaction (1) involves a loss of Na_2O (and CaO) and a gain of K_2O, whereas reaction (2) involves a loss of K_2O and gains in FeO and MgO, on the basis of constant Al_2O_3. The alteration is a useful means for discriminating geochemical trends due to diagenetic alteration from those due to hydrothermal alteration directly related to sulfide ores (Fig. 6a, b). The lamprophyre samples plot in the hydrothermal alteration field, particularly close to reaction No. 4: chlorite-carbonate alteration was typically developed, immediately adjacent to massive sulfide lenses. While cataclastic rocks are restricted to diagenetic alteration trend No.9: K-feldspar-albite-early diageneric trend of K-feldspar replacing albite (Gifkins and Allen, 2001).

The positive correlations (Fig. 7) for cataclastic, lamprophyre and wall-zone samples may suggest that the strong U-enrichment is due to post-magmatic processes. Moreover, the U-Zr/U, U-Ce/U diagrams (Fig. 7) show negative correlations, confirming U-enrichment in both cataclastic and shear-zone samples. The Th-eU/eTh, Th-Zr/Th and Th-Ce/Th diagrams show negative correlations, indicating that the U-bearing solutions are rich in Th.

5 Conclusions

(1) From the field observation of the three shear

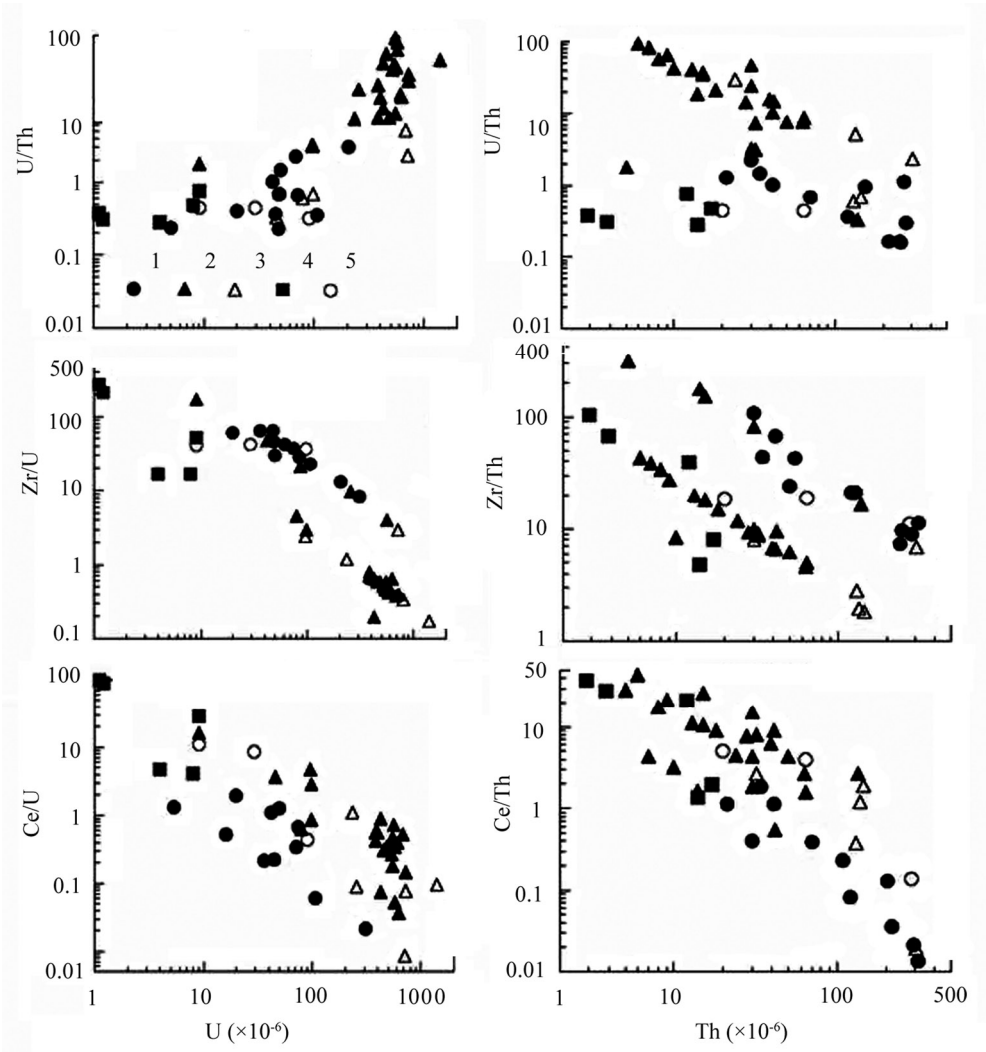

Fig. 7. Variation diagram of U vs. U/Th, Zr/U and Ce/U and Th against U/Th, Zr/Th and Ce/Th of cataclastic rocks, lampropyres, younger granites, wall zone and core samples, Abu Rusheid area, SED, Egypt. ● Cataclastic rock; ▲ lamprophyre sample; △ wall zone; ■ granite; ○ core sample.

zones, alteration processes and mineral identification, we can conclude that the Abu Rusheid area was affected by two or polycyclic tectonic processes, as reflected in faults and shear zones. The NNW-SSE faults along the shear zones themselves (including the first and second shear zones) were firstly formed and acted as channel ways for the movement and gathering of hydrothermal fluids. The ENE-WSW faults were formed later (the third shear zone), as reflected in the first and second shear zones, and also acted as channel ways for the movement and gathering of hydrothermal fluids. Therefore, the first two shear zones are believed to have experienced more intensive alteration, brecciation and mineralization than the third shear zone.

(2) The Abu Rusheid area was affected by numerous alteration processes represented by alkali metasomatism (sodic and potassic metasomatism), sericitization, argillation, greisenation, silicification, ferrugination, fluoritization, reduction, oxidation and carbonitization.

(3) Due to these alteration processes and the influence of hydrothermal solutions, a lot of mineralization has been formed. The mineralization brought about the primary uranium minerals (U_3O_8) and secondary U-minerals (uranophane and beta-uranophane, kasolite, torbernite, autunite and meta-autunite, astrocyanite, betafite and fergusonite), pyrite, iron oxides, zinc-manganese minerals (Mn-frankilinite and woodruffite), and some associated minerals (xenotime, allanite, zircon and cassiterite) (Fig. 8).

(4) The presence of different mineral parageneses with various alterations in the study area indicates that these rocks were subjected to the influence of acidic and alkaline minilizing solutions.

(5) The first and second shear zones have experienced much stronger alteration and mineralization than the third shear zone.

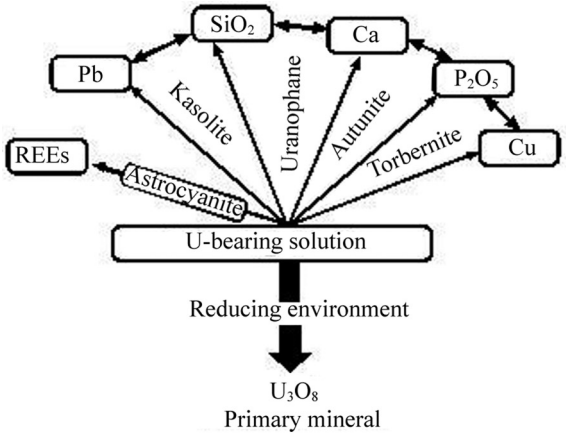

Fig. 8. Sketch diagram showing the mode of formation for secondary and primary uranium minerals in the Abu Rusheid area, SED, Egypt.

(6) The lamprophyres played an important role with hydrothermal solutions and alterations in the concentration and formation of minerals in the shear zones. During the extrusion of lamprophyres in the host rocks, the temperature was very high, causing the rocks to be heated. This heating process let many trace elements become free from their accessory minerals and mobilized through foliation, joints, fractures and shear zones in addition of alteration processes in the shear zones due to hydrothermal solutions (also rich in some elements, especially Cu, Y, Pb, W, V, Zn and U). The lamprophyres were formed from magmas which were enriched in carbon dioxide. The carbon dioxide is characterized by high fixation of all mineralization. Uranium is commonly seen along the brecciated shear zone, and has been completely altered to clay minerals. So the lamprophyres are considered as a chemical trap for mineralization.

(7) The U-bearing solutions resulted from leaching or ascending hydrothermal solutions (oxidizing environments). The leaching means that uranium was transported as uranyle (U^{6+}) by circulating ground waters from the surrounding granitic rocks. Whereas the ascending hydrothermal solutions carried the uranium as uranyle from the deep parts, where U^{4+} was oxidized into highly soluble uranyle (U^{6+}) and deposited mainly in the fractures, faults and shear zones. The U_3O_8 resulted from descending U-bearing solutions derived from meteoric waters until reaching reducing environment under high temperature conditions. The U_3O_8 was formed by reduction of the earlier-formed uranyle phase (dehydrated schoepite, UO_3 0.8 H_2O). While the secondary uranium minerals were formed from combination of U-bearing solutions with other cations such as Cu^{2+}, Ca^{2+}, Pb^{2+} and anions such as P_2O_5 and SiO_2. Uranium minerals, primary (U_3O_8) and secondary -bearing solutions were combined with REE to form (torbernite, autunite, uranophane, kasolite and astrocyanite) (Fig. 8), and REEs, tin, zinc, vanadium, gallium and copper are in association with clay minerals.

References

Creasy S.C. (1959) Some phase relations in the hydrothermal altered rocks of porphyry copper deposit [J]. *Econ. Geol.* **54**, 351–373.

Date J., Watanabe Y., and Saeki Y. (1983) Zonal alteration around the Fukazawa Kuroko deposits, Akita Prefecture, northern Japan [J]. *Econ. Geol*. **5**, 365–386.

Eastoe G.J., Solomon M., and Walshe J.L. (1987) District-scale alteration associated with massive sulfide deposits in the Mount Read Volcanic, western Tasmania [J]. *Econo. Geol.* **82**, 1239–1258.

Eid A.S. (1986) *Mineralogy and Geochemistry of Some Mineralized Rocks in Wadi El Gemal, Eastern Desert, Egypt* [D]. pp.165. Ph. D. Thesis, Ain Shams Univ.

El-Gemmizi M.A. (1984) On the occurrence and genesis of mud zircon in the radioactive psammitic gneisses of Wadi Nugrus, Eastern Desert, Egypt [J]. *J. Univ. Kawait* (Sci.). **2**, 285–294.

Gifkins C.C. and Allen R.L. (2001) Textural and chemical characteristics of diagenetic and hydrothermal alteration in glassy volcanic rocks: Examples from the Mount Read volcanics, Tasmania [J]. *Economic Geol*. **96**, 973–1002.

Hassan M.A. (1964) *Geology and Petrographical Studies of the Radioactive Minerals and Rocks in Wadi Sikait-Wadi El Gemal Area. Eastern Desert, Egypt* [M]. pp.165. M. Sc., Cairo Univ.

Hassan M.A. (1973) Geology and geochemistry of radioactive columbite-bearing psammitic gneiss of Wadi Abu Rusheid. South Eastern Desert, Egypt [Z]. *Annals of Geol. Surv. Egypt*. **VIII**, 207.

Ibrahim M.E., Assaf H.S., and Saleh G.M. (2000) Geochemical alteration and spectrometric analysis in Abu Rusheid altered uraniferous gneissose granites, South Eastern Desert, Egypt [J]. *Chem. Erde*. **60**, 173–188.

Ibrahim M.E., Saleh G.M., Amer T., Mahmoud F., Abu El Hassan A., Ibrahim I., Ali M., Azab M.S., Rashed M., Khaleal F., and Mahmoud M. (2004) *Uranium and Aassociated Rare Metals Potentialities of Abu Rusheid Brecciated Shear Zone II, Southeastern Desert,Egypt* [R]. pp.120. Internal report, Nuclear Materials Authority.

Ishikawa Y., Sawagushi T., Jwaya S., and Horiuchi M. (1976) Delineation of prospecting targets for Kuroko deposits based on modes of volcanism of underlying dacite and alteration holes [J]. *Mining Geol*. **26**, 105–117.

Large R.R., Gemmell J.B., and Paulik H. (2001) The alteration Box Plot: A simple approach to understanding the relationship between alteration mineralogy and lithogeochemistry associated with volcanic-hosted massive sulfide deposits [J]. *Econo. Geol*. **96**, 957–971.

Lentz D.R. (1999) Petrology, geochemistry, and oxygen isotope interpretation of felsic volcanic and related rocks hosting the Brunswick 6 and 12 massive sulfide deposits (Brunswick belt) Bathurst mining camp, New Brunswick, Canada [J]. *Econo. Geol*. **94**, 57–86.

Manning D.C. (1981) The effect of fluorine on liquids phase relationships in the system Qz-Ab-Or with excess water at 1 kb [J]. *Contib. Miner. Petrol.* **76,** 206–215.

Meyer C. and Hemley J.J. (1967) *Wall Rock Alteration in Geochemistry of Ore Deposits* (ed. H.L. Barnes) [M]. pp.166–235. New York.

Sabet A.H., Tsogoev V.B., Bordonosov V.P., Shoblovsky R.G., and Kossa M. (1976) On the geologic structures, laws of localization and prospects of Abu Rusheid rare metals deposit [Z]. *Annals of Geol. Surv. Egypt*. **VI**, 181–197.

Saleh G.M. (1997) *The Potentiality of Uranium Occurrences in Wadi Nugrus Area, South Eastern Desert, Egypt* [D]. pp.171. Ph. D. Thesis, Mans. Univ.

Stempork M. (1979) Mineralization granites and their origin [J]. *Episodes*. **3**, 20–24.

Tuttle O.F. and Bowen N.L. (1958) Origin of granite in the light of experimental studies in the system $NaAlSi_3O_8$-$KAlSi_3O_8$-SiO_3-H_2O [J]. *Geol. Soc. Am. Mineral*. **74**, 153.